Fast ion transport in TORPEX: framework for comparison between theory and experiment

K. Gustafson, A. Bovet, A. Fasoli, I. Furno, P. Ricci

Ecole Polytechnique Fédérale de Lausanne (EPFL), Centre de Recherches en Physique des Plasmas, Association Euratom-Confédération Suisse, CH-1015 Lausanne, Switzerland

Fundamental aspects of the transport of fast ions in ideal interchange-mode turbulence are investigated in the simple magnetized torus (SMT), an open field line configuration with a vertical magnetic field, B_v, combined with a toroidal magnetic field, B_ϕ. We follow fast ion tracer trajectories using the full Lorentz force specified by electrostatic turbulence from a numerical simulation based on the drift-reduced Braginskii equations in two dimensions [1].

This work is inspired by fast ion experiments in TORPEX [2], in which the spatial profile of a lithium ion beam injected nearly parallel to the magnetic field lines is resolved using a gridded energy analyzer. TORPEX is an example of an SMT with major radius 1 m and minor radius 20 cm. The toroidal magnetic field at the center of the torus is $B_\phi \sim 100$ mT and the vertical field is $B_v \sim 1$ mT. For sufficiently large values of B_v, the turbulence is dominated by the $k_\parallel = 0$ ideal interchange mode [3].

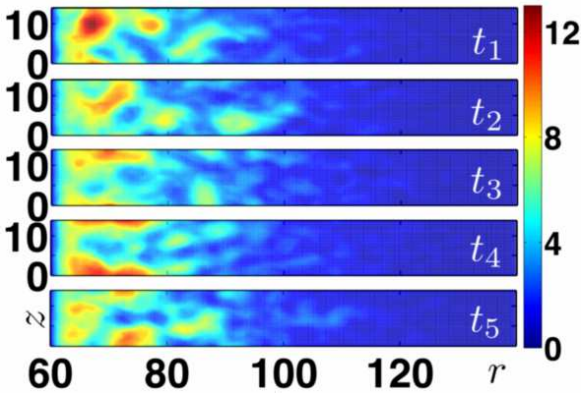

Figure 1: Electrostatic potential $\Phi(r,z)$ in nonlinear regime of interchange turbulence in the $k_\parallel = 0$ GBS simulation of a TORPEX-like SMT with a minor radius $r_0 = 40$ cm and a vertical field-line return distance $\Delta = 14$ cm. These six snapshots are at sequential times, t_i, such that $t_{i+1} - t_i \sim 330\,\tau_L$, where $\tau_L = \frac{2\pi}{\Omega_{fi}}$.

Therefore, a two-dimensional simulation in this regime (see Fig. 1) provides a turbulent electrostatic potential, $\Phi(r,z,t)$, into which fast ions are injected. Similarly to the experiment [4], the simulated plasma can be divided into a coherent mode region, on the high-field side of the SMT where the plasma is generated, and an intermittent blob region on the low-field side. The ion motion is simulated in three-dimensions, though there are no forces in the field-line-following $\hat{b}$ direction since $k_\parallel = 0$. The amplitude of the simulated electrostatic potential fluctuations, $\Phi = \Phi_0 + \xi\,(\Phi - \Phi_0)$, can be scaled *a posteriori* by a factor ξ, where Φ_0 is t and z-averaged. We emphasize that the turbulence simulation is full-n, since the equilibrium and fluctuations are of the same order in the experiment.

Trajectories of ions under the influence of the Lorentz force can often be approximated by

a combination of Larmor motion, $\mathbf{E}\times\mathbf{B}$ drifts ($\mathbf{v}_{E\times B}$), and the $\nabla\mathbf{B}$/curvature drifts ($\mathbf{v}_{SMT}$) in the toroidal geometry, shown in Fig. 2. All of the drifts mentioned here have been identified individually in the simulations. As a complement to the SMT simulations, we also simulate fast ions in the same turbulence in a "slab" geometry. The slab has straight, uniform magnetic field lines (eliminating $\mathbf{v}_S MT$ drifts) and is also relevant in linear devices such as LAPD [5]. To examine how these drifts determine the dispersion of the population of ions injected nearly parallel to the magnetic field, we use experimentally relevant initial distributions of injection angle and energy, mimicking the TORPEX fast ion source [6].

The main diagnostic for transport of fast tracer ions in turbulence is the distribution of ion displacements $\delta r_i = r_i(t) - r_i(0)$ where i is the fast ion index. We concentrate on the variance of the displacements (second moment of the distribution)

$$\sigma_r^2(t) = \left\langle (\delta r_i - \langle \delta r_i \rangle)^2 \right\rangle \sim t^{\gamma_r}, \qquad (1)$$

where $<>$ is an ensemble average over many particle trajectories. The exponent γ characterizes whether the transport is subdiffusive ($\gamma < 1$), superdiffusive ($\gamma > 1$) or ballistic ($\gamma \sim 2$). Time is measured here in units of $\tau_L = 2\pi/\Omega_{fi}$. Examination of σ_r^2 in the SMT and slab geometry for ensembles of $N_{fi} = 10000$ Li^{+6} ions at various experimentally relevant injection energies $\mathscr{E}$ reveals distinct, sequential regimes for the dispersion rate for many experimentally relevant values of $\mathscr{E}$. Though the transitions between these phases are fairly smooth, it is possible to categorize them distinctly. They could be called (1) ballistic from the injection to the point in time when the velocity is modified substantially by the fields, (2) intermediate when a quasi-steady value of γ is reached and (3) asymptotic when the value of γ reaches a second steady state.

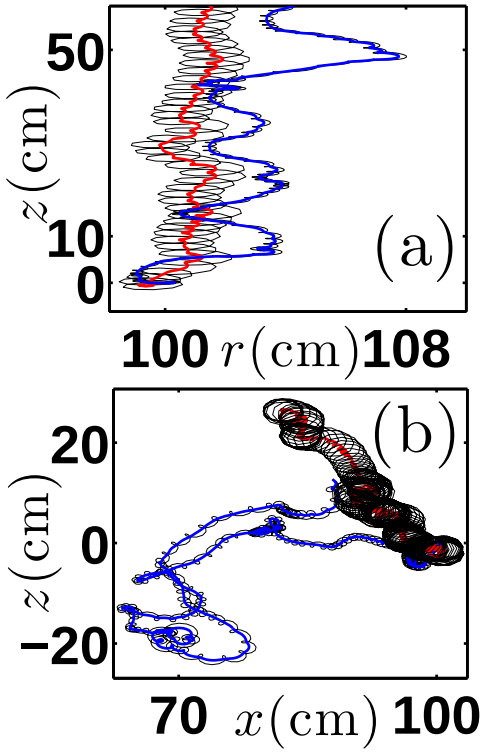

Figure 2: Trajectories of lithium ions in the perpendicular plane with particles (thick black line) and corresponding gyrocenters for high (red) and blue (low) energy. Distances are measured in cm. In (a), using an SMT field for $\mathscr{E} = 40$ eV and $\mathscr{E} = 100$ eV. In (b), using a slab field for $\mathscr{E} = 200$ eV and $\mathscr{E} = 2000$ eV.

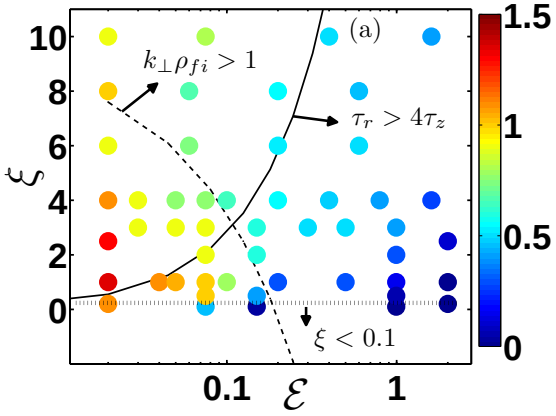

Figure 3: Phase space scan for dispersion exponent γ_r, (colored dots) in $(\mathscr{E}(keV), \xi)$ space. Generally, γ becomes diffusive when $k_\perp \rho_{fi} > 1$ (dashed curve). Below $\xi \sim 0.1$ (dotted line), the turbulent fluctuations are too small for connected radial streamlines to form, therefore $\gamma \to 0$. The boundary for subdiffusive trapping due to $\mathbf{v}_{SMT}$ is shown (solid black curve), where τ_r and τ_z are the typical eddy crossing times.

The ballistic phase is a relatively short period, when $\gamma_r \sim 2$, before the ions interact significantly with the turbulence. In the intermediate phase, $\gamma_r \neq 1$ generally. This transport can be superdiffusive $\gamma_r > 1$ or subdiffusive $\gamma_r < 1$ depending on $\mathscr{E}$ and ξ, as shown in Fig. 3. In the asymptotic phase, which is only relevant to large $\mathscr{E}$ where the intermediate phase is subdiffusive, $\gamma \to 1$, but the dispersion is asymmetric, biased towards the mode region.

These results can be applied to TORPEX, noting that the comprehensive analysis of fast ion behavior given here is valid for time and length scales longer than those accessible by the experiment. The timeframe for measuring the intermediate and asymptotic phases is limited by the toroidal connection length of the field lines, by the vertical distance through which ions can follow $\mathbf{v}_{SMT}$ before colliding with the vessel, and by the radial distance through which ions can follow $\mathbf{v}_{E\times B}$ before reaching the vessel wall. An experimentally accessible intermediate phase for $\mathscr{E} = 100$ eV is shown in Fig. 4, where the radial and vertical spreading can be measured to be subdiffusive and superdiffusive, respectively, at a source-detector separation of 100 cm.

To observe the transition from the ballistic phase to the subdiffusive phase, the toroidal resolution of the measurements should be 0.5 cm^{-1} in order to see the Larmor oscillations. This toroidal resolution will be possible with the future use of the recently built toroidally moveable system, mounted on the vacuum vessel [7].

The first data point from the TORPEX fast ion diagnostic is in the predicted ballistic phase, with source and detector at 25 cm toroidal separation. This single point in $R\phi$ is not sufficient to determine γ, but a comparison for the order

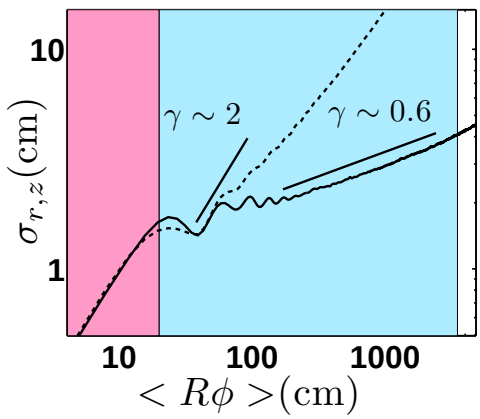

Figure 4: Radial (solid curve), σ_r and vertical σ_z (dashed curve) standard deviation (in cm) of $\mathscr{E} = 100$ eV fast ion displacements for TORPEX, showing power laws (line segments) for $\sigma \sim t$ (ballistic, red) and $\sigma \sim t^{0.2}$ (subdiffusive, blue).

of magnitude turbulent spreading caused by the TORPEX plasma and the simulated GBS plasma is possible. We use a synthetic diagnostic to compare with experimental ion current profiles. The synthetic ion current is composed of the integrated product of the ion density and velocity at a specified toroidal location. Radial spreading of the profile increases by $\sigma_r \sim 10\%$ at $\langle R\phi \rangle = 25$ cm for a turbulent, ideal interchange-mode plasma. The synthetic diagnostic and TORPEX experiment agree on this measurement of spreading at the single toroidal location, as shown in Fig. 5. New measurements at several toroidal locations will soon be available.

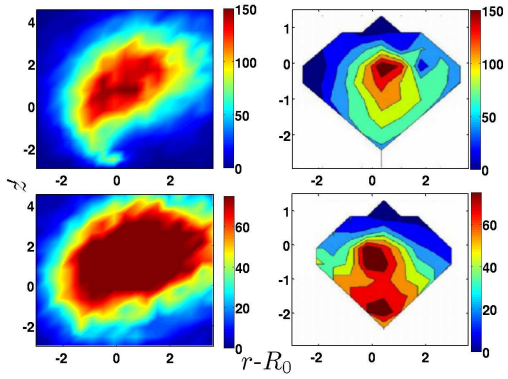

Figure 5: Synthetic diagnostic for the fast ion current and data from the TORPEX fast ion diagnostic. The radial spreading of the fast ions with the presence of plasma is approximately 10% larger than without plasma.

We are pleased to acknowledge funding from the United States National Science Foundation International Research Fellowship Program and the Fonds National Suisse de la Recherche Scientifique.

References

[1] P. Ricci and B. N. Rogers, Physical Review Letters **104**, 145001 (2010).

[2] A. Fasoli, B. Labit, M. McGrath, S. H. Müller, G. Plyushchev, M. Podestà and F. M. Poli, Physics of Plasmas **13**, 055902 (2006).

[3] P. Ricci and B. N. Rogers, Physics of Plasmas **16**, 062303 (2009).

[4] I. Furno, B. Labit, A. Fasoli, F. M. Poli, P. Ricci, C. Theiler, S. Brunner, A. Diallo, J. P. Graves, M. Podestà, and S. H. Müller, Physics of Plasmas **15**, 055903 (2008).

[5] S. Zhou, W. W. Heidbrink, H. Boehmer, R. McWilliams, T. Carter, S. Vincena, S. K. P. Tripathi, P. Popovich, B. Friedman, and F. Jenko, Physics of Plasmas **17**, 2103 (2010).

[6] G. Plyushchev, A. Diallo, A. Fasoli, I. Furno, B. Labit, S. H. Müller, M. Podestà, F. M. Poli, H. Boehmer, W. W. Heidbrink, and Y. Zhang, Review of Scientific Instruments **77**, 10F503 (2006).

[7] A. Fasoli, A. Burckel, L. Federspiel, I. Furno, K. Gustafson, D. Iraji, B. Labit, J. Loizu, G. Plyushchev, P. Ricci, C. Theiler, A. Diallo, S. H. Mueller, M. Podestà, and F. Poli, Plasma Physics and Controlled Fusion **52**, 124020 (2010).